Theor Chem Acc (2011) 130:1023–1030
DOI 10.1007/s00214-011-0986-9

REGULAR ARTICLE

D_{3h} Al_3N: a novel promising ligand for coordination chemistry

Nan Li · Qiong Luo

Received: 14 January 2011 / Accepted: 24 June 2011 / Published online: 13 July 2011

Abstract Several prior experimental and theoretical studies have been reported on Al_3N and have shown that the D_{3h} isomer is the global minimum. In this work, we attempt to theoretically design new molecular materials containing the D_{3h} Al_3N as unit. A novel series of metal complexes with the Al_3N ligand, including $[(Al_3N)K(Al_3N)]^+$ (traditional homo-decked sandwich), $[(Al_3N)ZnZn(Al_3N)]^{2+}$ (binuclear metallocene), and $[(Al_3N)Zn(C_5H_5)]^+$ (hetero-decked sandwich), are predicted to be local minima on their corresponding potential hyper surfaces at the B3LYP, B3PW91, and BP86 levels of theory with the 6–311+G(d) basis set. Natural bond orbital and AOMix analyses indicate that the interaction between the metal ions and the Al_3N ligands is mostly electrostatic. This fact suggests that the Al_3N is a promising ligand for coordination chemistry.

Keywords Al_3N · Binuclear metallocenes · Hetero-decked sandwich compound · Compound of Zn(I)

Dedicated to Professor Akira Imamura on the occasion of his 77th birthday and published as part of the Imamura Festschrift Issue.

Electronic supplementary material The online version of this article (doi:10.1007/s00214-011-0986-9) contains supplementary material, which is available to authorized users.

N. Li · Q. Luo (✉)
State Key Laboratory of Explosion Science and Technology, Beijing Institute of Technology, Beijing 100081, People's Republic of China
e-mail: kellyluo@bit.edu.cn

Q. Luo
Center for Computational Quantum Chemistry, South China Normal University, Guangzhou 510631, China

N. Li
School of Life Science, Beijing Institute of Technology, Beijing 100081, People's Republic of China

N. Li
Institute of Chemistry Chinese Academy of Science, Beijing 100190, People's Republic of China

1 Introduction

Stable cluster species have drawn a great deal of attentions, because the cluster-assembled materials could possess fancy and peculiar properties [1, 2]. Ideally, these clusters would ultimately retain their structural integrity upon complexation, thereby making them suitable as building blocks in synthesizing new tailor-designed materials [3–7]. The Jellium model is a theory to provide the simplest approximation for searching stable metallic clusters. In this model, the clusters containing 2, 8, 18, 20… filled valence electrons always have particular stabilities [8–11]. However, this simple picture is not suitable for small-size clusters we are interested in this study. Aromaticity, which refers to the specific stabilities of cyclic planar molecules, should be a valuable starting point for searching stable small-size clusters, especially since the applications of aromaticity have been extended to the heterosystems, organometallic compounds, and all-metal systems [12].

Recently, a number of nitrogen-doped aluminum clusters have been reported [13–15], among which, Al_3N has attracted extensive concentrations because its global minimum possesses unique properties: close-shelled electronic configuration, planarity, and high symmetry of D_{3h} [13–19]. The D_{3h} Al_3N is isoelectronic with $[Al_3H_3]^{2-}$ which belongs to the family of $[Al_3R_3]^{2-}$ (R=H, F, and CF_3 and so on), a new family of aromatic ligands for metal coordination complexes [20, 21]. The theoretical studies on

this family revealed that these dianions possessed one σ-type and one π-type independent delocalized bonding systems which both satisfied the $4n + 2$ electron counting rule of aromaticity and could form sandwich complexes containing metals and metal dimers without losing their individual integrity. Thus, these $[Al_3R_3]^{2-}$ ions have become the perfect candidates as building blocks for cluster assembly [21].

For the D_{3h} Al_3N species, the central N atom provides three sp^2 hybrid orbitals to form three inner single bonds with the Al_3 ring which correspond to the three Al–H bonds in $[Al_3H_3]^{2-}$. Also, considering the planarity and high stability of the D_{3h} Al_3N, one can speculate that the residual two $p_z - \pi$ electrons of the N atom delocalize over the whole molecule as in the case of the two excessive electrons in $[Al_3H_3]^{2-}$. The similarity of the electronic properties between the D_{3h} Al_3N and $[Al_3H_3]^{2-}$ arouses our interests in exploring the possibility of the D_{3h} Al_3N to be a unit for molecular assembly. To the best of our knowledge, no Al_3N-based assembled molecular compounds have been reported. In this paper, we considered an important strategy "sandwiching", which is probably the most powerful one for assembly and growth of a stable small unit into more complex compounds. Three types of sandwich compound containing the Al_3N ligands were theoretically constructed.

2 Computational methods

All calculations for geometry optimization and frequency analysis were performed by the B3LYP functional [22, 23], which is a widely used and accepted tool for the prediction of ground state molecular properties. Recent studies have shown that the B3LYP is not reliable enough to treat dispersion interactions and to estimate the transition energies for charge transfer electronic-excited state transitions [24–27]. Thus, comparison calculations with the B3PW91 [22, 28] and BP86 [29, 30] functionals were performed. For all the cases, the 6–311+G(d) basis set [31] was used. The geometry parameters obtained from the three methods are very close to each other, especially for those predicted at the B3LYP and B3PW91 levels of theory. The B3LYP results were mainly discussed in the text. The stabilities of the sandwich molecules were examined by the means of fragmentation. The free energy of solvation (ΔG_{solv}) of these sandwich species in water and dichloromethane were predicted by the polarizable continuum (PCM) calculations [32, 33] at the B3LYP/6–311+G(d) level of theory. The details of the used PCM model in this study are that: (1) the radii for the spheres centered on the atoms are specified by the UAHF model; (2) the overlap index between two interlocking spheres is set to 0.89; (3) the minimum radius for the added sphere to smooth the solvent excluding surface is set to 0.2 Å. In addition, the reaction energies of the fragmentation reactions were presented where the same solvent model were taken into account. All the calculations were carried out by using Gaussian 03 program [34]. The bonding patterns of the complexes were explored by the AOMix [35, 36] and NBO 5.0 [37] packages based on the structures predicted at the B3LYP/6–311+G(d) level of theory.

3 Results and discussion

3.1 Evidence of the aromaticity of the D_{3h} Al_3N

Analysis of the calculated valence molecular orbitals is an admitted method for understanding aromaticity or antiaromaticity. Figure 1 shows an orbital correlation diagram of the interactions between the N atom and the Al_3 ring. The σ-type valence MOs in the D_{3h} Al_3N can be divided into three groups: (1) the three lowest-lying occupied bonding orbitals (HOMO-4 and degenerate HOMO-3) mainly consisted of the sp^2 hybrid orbitals of the N atom; (2) the nonbonding orbital (HOMO-1) with dominating contribution of 3*s* orbitals of the Al atoms; (3) the degenerate antibonding orbitals (HOMO) greatly composed of 3*s* orbitals of the Al atoms. Obviously, in the D_{3h} Al_3N, there are no σ-type MOs delocalizing over the whole molecule. However, in the isoelectronic $[Al_3H_3]^{2-}$, there is a a_1' radial MO which is a delocalized bonding system and results in σ-aromaticity for the $[Al_3H_3]^{2-}$ [20, 21]. This orbital is very similar to HOMO-1 in the D_{3h} Al_3N. The inner coordination of the N atom to Al_3 ring substantially stretches the Al_3 ring, for instance the calculated Al–Al bond distance in the D_{3h} Al_3N of 3.204 Å much longer than those in $[Al_3H_3]^{2-}$ of 2.522 Å at the B3LYP/6–311+G(d) level of theory, and prevents the radial system (HOMO-1) from delocalizing over the whole Al_3 ring.

The HOMO-2 orbital of the D_{3h} Al_3N is a classic π orbital with 97% contribution from the N p_z orbital. As shown in Fig. 1, it delocalizes over the whole molecule and displays the typical pattern of a two-π-electron, Hückel, aromatic system, indicating that the D_{3h} Al_3N exhibits the traditional (organic) aromaticity.

3.2 Possibility of the D_{3h} Al_3N assembly

It is worth noticing that the D_{3h} structure is the most stable isomer for Al_3N. The structural stability and aromatic character of the D_{3h} Al_3N make it a potentially stable metal-complexation ligand for organometallic chemistry. However, it is a challenge to obtain Al_3N-based

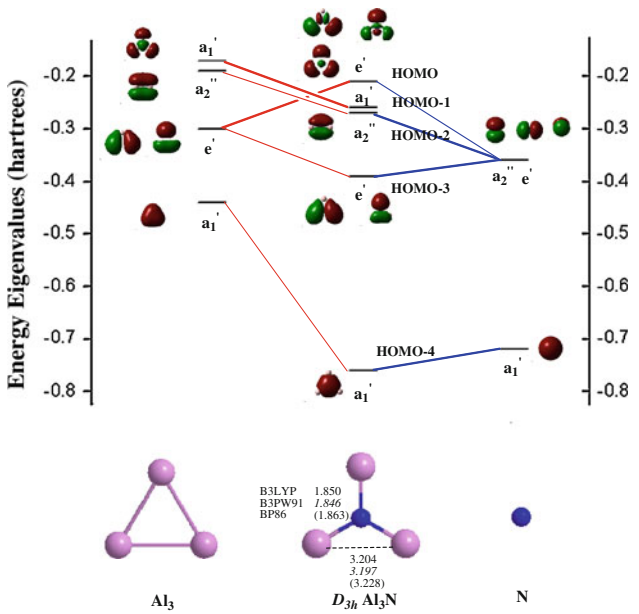

Fig. 1 The valence orbitals of D_{3h} Al_3N, Al_3, and N (with an isosurface contour value of 0.03) and orbital interaction diagram for the D_{3h} Al_3N formed by Al_3 and N

coordination complexes because of the tendency of forming additional Al–Al bond between Al_3N species during complexation [38]. To resolve this problem, two strategies were proposed as following to protect aluminum atoms from collapsing: (1) separating the ligands far apart from each other by metals with longer atomic radius or metal dimers in the traditional "homo-decked sandwich" form (2) using "hetero-decked sandwich" scheme.

Traditional homo-decked sandwich compounds, binuclear metallocene, and hetero-decked sandwich compounds were designed. The natural atomic charge on the central N atom of the D_{3h} Al_3N is −2.46 e (Table 1), implying that the Al_3N deck should preferentially interact with the metal cations along the threefold axis by ionic interaction. The alkali metal K was selected to assembly the D_{3h} Al_3N in the traditional "homo-decked sandwich" growth pattern because of its large ionic radius and electropositivity. The compounds, $[(Al_3N)ZnZn(Al_3N)]^{2+}$ and $[(Al_3N)Zn(C_5H_5)]^{+}$, were constructed as example of binuclear metallocene and hetero-decked sandwich, respectively.

The overviews of the structures and selected bond lengths for the three kinds of designed compounds are depicted in Fig. 2. As well, Table 1 collects the lowest vibrational frequencies (ν_{min}), natural atomic charges, and selected Wiberg bond indices (WBI) for these compounds. The B3LYP, B3PW91, and BP86 atomic coordinates for all the structures are provided as Electronic Supplementary Material.

3.2.1 *Homo-decked sandwich compounds based on the D_{3h} Al_3N*

3.2.1.1 $[(Al_3N)K(Al_3N)]^+$ Figure 2 shows the optimized D_{3d} staggered and D_{3h} eclipsed $[(Al_3N)_2K]^+$ structures. The two structures have nearly same energies, which suggest that there is a free rotation around the C_3 axis. The flatness of the potential energy surface (PES) with respect to this rotational motion is also fully appreciated by the small values of the lowest normal modes of the D_{3d} and D_{3h} $[(Al_3N)_2K]^+$ (Table 1). In the both $[(Al_3N)_2K]^+$ structures, the parallel Al_3N rings are separated by a distance of ~6.1 Å and nearly have the same structure as the isolated D_{3h} Al_3N.

The NBO analyses were executed to explore the main feature of the interaction between K^+ and Al_3N. The WBI of the K–N bond ($WBI_{K-N} = 0.01$, Table 1) indicates that the bond between the K^+ and Al_3N is mainly ionic. The stabilities of the predicted molecules are checked by fragmentation. Table 2 shows that the dissociation energy for $[(Al_3N)_2K]^+ \rightarrow 2Al_3N + K^+$ is 12.3 kcal/mol. The Gibbs free energy ($\Delta_r G$) of the fragmentation reaction was also calculated by the B3LYP method at 298 and 223 K, respectively. The value of $\Delta_r G$ at 298 K ($\Delta_r G_{298\ K}$) is −0.1 kcal/mol, while the value at 223 K ($\Delta_r G_{223\ K}$) increases to +2.8 kcal/mol. This implies that the D_{3d} $[(Al_3N)_2K]^+$ species could only be experimentally observed at low temperature.

3.2.1.2 $[(Al_3N)ZnZn(Al_3N)]^{2+}$ The discovery of the first dimetallocene, $(\eta^5 - Me_5C_5)_2Zn_2$, must be one of the most exciting recent developments in organometallic chemistry [39]. Sequentially, the binuclear metallocenes as a novel kind of extended metallocene opened a new set of research targets [40]. Additional benefit of sandwiching metal dimers is that the spacers between the two cyclotrialane ligand rings could separate the rings apart as far as possible, therefore preventing the aluminum atoms from aggregating.

The D_{3d} structure of $[(Al_3N)ZnZn(Al_3N)]^{2+}$ has one imaginary frequency of 1i cm^{-1} (Table 1). Schaefer has pointed out that low magnitude imaginary vibrational frequencies are suspected because the numerical integration procedures used in existing DFT methods have significant limitations. Thus, an imaginary vibrational frequency of magnitude <100i cm^{-1} should imply that there is a minimum with energy very similar to that of the stationary point in question. In most cases, we do not follow the eigenvectors corresponding to imaginary frequencies less than 100i cm^{-1} to search of another minimum [41, 42]. Therefore, the structure of D_{3d} $[(Al_3N)ZnZn(Al_3N)]^{2+}$ could still be identified as a local minimum.

Table 1 Lowest vibrational frequencies (cm^{-1}), natural atomic charges (q) of N atoms and sandwiched metal atoms, and Wiberg bond indexes (*WBI*) of selected bonds of all the complexes studied in the present article, predicted at the B3LYP/6–311+G(d) level of theory

Species	ν_{min}	q_N	q_M	WBI_{M-N}	WBI_{Zn-Zn}
D_{3h} Al_3N	153	−2.46			
D_{3d} $[(Al_3N)K(Al_3N)]^+$	6	−2.52	0.88	0.01	
D_{3h} $[(Al_3N)K(Al_3N)]^+$	2i	−2.52	0.88	0.01	
D_{3d} $[(Al_3N)ZnZn(Al_3N)]^{2+}$	1i	−2.64	0.83	0.15	0.68
D_{3h} $[(Al_3N)ZnZn(Al_3N)]^{2+}$	1	−2.64	0.83	0.15	0.68
C_s $[(Al_3N)Zn(C_5H_5)]^+$	13	−2.59	1.55	0.26	

M sandwiched metals

The difference of energies between D_{3d} and D_{3h} $[(Al_3N)ZnZn(Al_3N)]^{2+}$ conformations is negligible, implying that the transfer happening on the rotational path is automatic. Therefore, one of the rotational isomers could be employed to descript the sandwich-type complexes $[(Al_3N)ZnZn(Al_3N)]^{2+}$. Here, we only chose D_{3d} $[(Al_3N)ZnZn(Al_3N)]^{2+}$ structure to discuss in terms of geometry and bonding mechanism.

The distance between the two Al_3N ligands is 6.4 Å, which is long enough to avoid the collapse of the ligands. The optimized Zn–Zn bond distance of 2.433 Å, is a bit longer than the ones in other dizinc species. For instance, the Zn–Zn distance in Cp*Zn–ZnCp* (Cp*=C_5Me_5) obtained by X-ray structure analysis is 2.305 (±3) Å [39] and the predicted Zn–Zn distances in Zn_2X_2 (X=H, F, Cl, Br, and I) lie in the range of 2.28–2.42 Å [43–45].

The MO analysis has been done by using the AOMIX program to understand the bonding mechanism in complex $[(Al_3N)ZnZn(Al_3N)]^{2+}$. Figure 3a shows that the higher-energy occupied orbitals (from HOMO to HOMO-3) are quasi-degenerate with major contribution from the e′ Al_3N orbitals. Figure 3b is the overlap population density of state (OPDOS) plot. In the district of occupied orbitals, two prominent bonding peaks of the Zn–Zn plot are relative to HOMO-6 and 4. The bonding interaction in HOMO-6 and 4 is σ-type with primary contribution from Zn 4*s* orbitals. A single bond displaying a nearly pure *s* character between Zn and Zn atoms is also suggested by the WBI_{Zn-Zn} of 0.70 and the $sp^{0.04}d^{0.00}$ hybridization of Zn. Although, the Zn–Zn bond distance in $[(Al_3N)ZnZn(Al_3N)]^{2+}$ is longer than the one in $(\eta^5-Me_5C_5)_2Zn_2$, there still exists a unique unit of Zn_2^{2+}. There is nearly no orbital overlap between Zn and Al_3N (Fig. 3b). The atomic charges of Zn and N are +0.83 and −2.64 e (Table 1), respectively, demonstrating the existence of the ionic bond between metal atom and ligand. Therefore, in the $[(Al_3N)ZnZn(Al_3N)]^{2+}$, the metal–ligand bond is ionic bond.

The stability of the D_{3d} $[(Al_3N)ZnZn(Al_3N)]^{2+}$ is estimated by the following fragmentation reactions: $[(Al_3N)ZnZn(Al_3N)]^{2+} \rightarrow [Zn_2(Al_3N)]^{2+} + Al_3N$ and $[(Al_3N)ZnZn(Al_3N)]^{2+} \rightarrow 2[Zn(Al_3N)]^+$. The dissociation energy ΔE is 55.8 kcal/mol for the first reaction and 7.4 kcal/mol for the second (Table 2), respectively. The Δ_rG for the first reaction is substantial. Table 2 shows that the values of Δ_rG are 43.0 and 46.2 kcal/mol at temperature 298 and 223 K, respectively. However, the Δ_rG values for the second reaction reveal that the process of $[(Al_3N)ZnZn(Al_3N)]^{2+}$ dissociating into two $[Zn(Al_3N)]^+$ radicals carries on spontaneously when the temperature is higher about −170 °C. Therefore, in the $[(Al_3N)ZnZn(Al_3N)]^{2+}$, the Zn-$NAl_3$ bond is much stronger than the Zn–Zn bond. The binuclear metallocene compound is thermodynamically unstable to dissociate to $[Zn(Al_3N)]^+$ radicals. Apparently, on one hand, trapping the $[(Al_3N)ZnZn(Al_3N)]^{2+}$ in lab is a large challenge. On the other side, the favored dissociation to produce $[Zn(Al_3N)]^+$ radicals suggests the stability of the radicals and the possibility of investigating the radicals. It is interesting to note that the $[Zn(Al_3N)]^+$ radical is a compound of Zn(I).

The first example of Zn(I) compound, decamethyldizincocene $(\eta^5-Me_5C_5)_2Zn_2$, was formally derived from the dimetallic $[Zn–Zn]^{2+}$ unit which was stabilized by the ligand of $[Me_5C_5]^-$[39]. The dissociation energy of Zn–Zn bond for $(\eta^5-Me_5C_5)_2Zn_2$ is around 66 kcal/mol [46, 47], which is considerable larger than that of 7.4 kcal/mol for $[(Al_3N)ZnZn(Al_3N)]^{2+}$. Thus, the D_{3h} Al_3N is not an appropriate ligand to form a stable compound of Zn(I) containing Zn–Zn bond. However, the thermodynamic stability of the $[Zn(Al_3N)]^+$ radical, as mentioned above, suggests that Al_3N is a potential ligand to stabilize Zn^+ cation. Moreover, the molecule structure of the C_{3v} $[Zn(Al_3N)]^+$ has no negative force constants. It seems that the C_{3v} $[Zn(Al_3N)]^+$ is a new species of Zn(I) compounds. The atomic coordinates for the C_{3v} $[Zn(Al_3N)]^+$ are provided as Electronic Supplementary Material.

3.2.2 *Hetero-decked sandwich compounds based on Al_3N*

Hetero-decked "*sandwiching*" is an effective strategy to incorporate some particular units into assembled molecular materials, especially, the units tending to self-fusion such

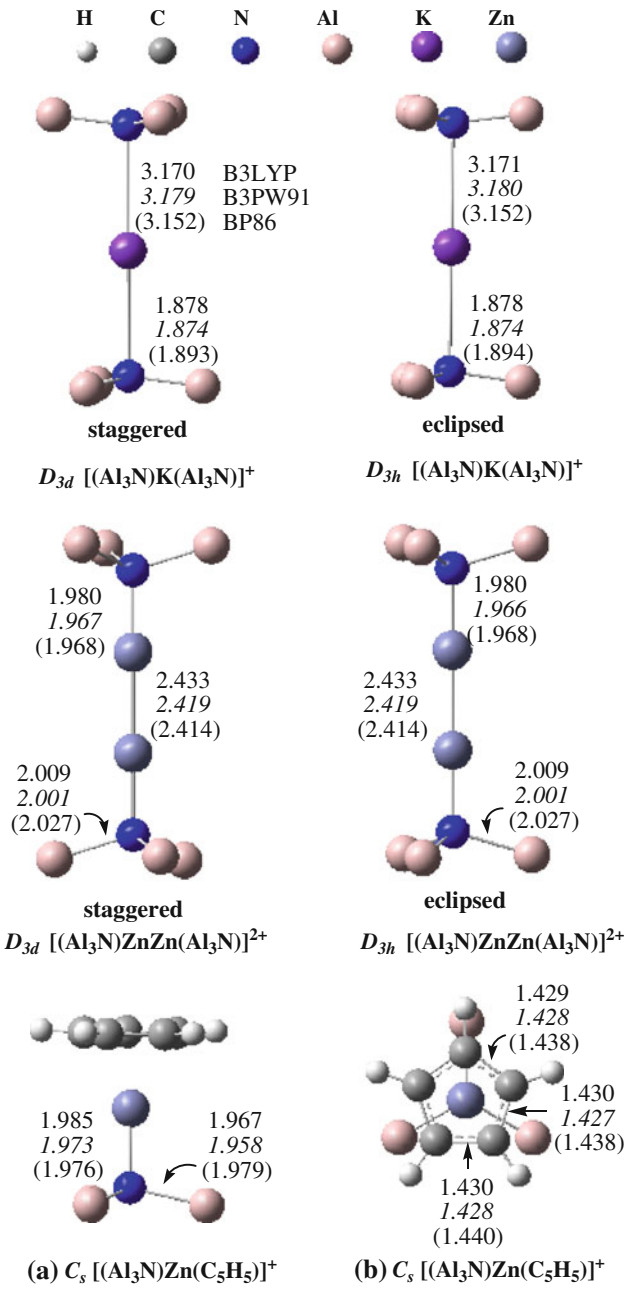

Fig. 2 Optimized geometries of *staggered* D_{3d} and *eclipsed* D_{3h} $[(Al_3N)K(Al_3N)]^+$, *staggered* D_{3d} and *eclipsed* D_{3h} $[(Al_3N)ZnZn(Al_3N)]^{2+}$ and C_s $[(Al_3N)Zn(C_5H_5)]^+$. The selected bond distances predicted by the B3LYP, B3PW91 (*italic*), and BP86 (in *parenthesis*) methods are given in Å. **a** and **b** are the structures of C_s $[(Al_3N)Zn(C_5H_5)]^+$ viewed from different perspectives

as small aluminum rings [48]. In this paper, the scheme for assembly of Al_3N unit in $[(Al_3N)Zn(C_5H_5)]^+$ was utilized.

As shown in Table 1 and Fig. 2, the optimized molecular structure of $[(Al_3N)Zn(C_5H_5)]^+$ has no negative force constants. The bond length of Zn-N in $[(Al_3N)Zn(C_5H_5)]^+$ is 1.984 Å which is close to the one in $[(Al_3N)ZnZn(Al_3N)]^{2+}$. The natural atomic charges on the N atom, Zn atom, and Cp units are −2.59, +1.55, and −0.70 e, respectively, which suggest that there are strong electronic interactions between Zn and the two ligands. Do covalent bonding interactions exist to bind the ligands to Zn metal in the $[(Al_3N)Zn(C_5H_5)]^+$? The OPDOS plot (Fig. 4) help to answer this question. It is shown in Fig. 4 that the bonding interaction peak of the Zn–Cp plot locates at the degenerate HOMO-2 and 3 orbitals which are consist of the e_1'' π–C_5H_5 orbitals (more than 95%) and the 4*p* orbitals of Zn. The bonding interaction between the Cp unit and Zn atom could be described as a π back-donation from the ligand to the central metal. When it comes to the Zn–NAl_3 plot, there are no clear bonding peaks, indicating that the interaction between Zn and Al_3N is a typical ionic bonding. Therefore, the electrostatic interactions between Zn and Cp unit as well as Zn and Al_3N ligand are the principal impetus to stabilize the $[(Al_3N)Zn(C_5H_5)]^+$, and the π back-donation between Zn and Cp unit also support the stabilizing.

Additional clue of the stability of the hetero-decked assembled compound $[(Al_3N)Zn(C_5H_5)]^+$ comes from the thermodynamic data of the fragmentation, $[(Al_3N)Zn(C_5H_5)]^+ \rightarrow (C_5H_5)^- + Zn^{2+} + Al_3N$. The ΔE and $\Delta_r G_{298\ K}$ of the dissociation are 493.6 and 473.3 kcal/mol, respectively, implying the strong thermodynamical feasibility of the reverse synthesis reaction.

3.3 Solvent effects of the three sandwich species in water and dichloromethane

Because the complexes of the D_{3d} $[(Al_3N)K(Al_3N)]^+$, D_{3d} $[(Al_3N)ZnZn(Al_3N)]^{2+}$ and C_s $[(Al_3N)Zn(C_5H_5)]^+$ are ionic species it would be good to test the effect of including a solvent model. For an example, the solvent effects of the three sandwich species in water and dichloromethane have been investigated by using the PCM model at the B3LYP/6–311+G* level of theory in terms of the free energy of solvation (ΔG_{solv}), which is the energy of transferring a molecule from the gas phase into solution, composed of three contributions: cavitation (ΔG_{cav}), van der Waals term (ΔG_{vw}), and electrostatic (ΔG_{elec}) free energies.

$$\Delta G_{solv} = \Delta G_{cav} + \Delta G_{vw} + \Delta G_{elec}$$

As shown in Table 3, the PCM calculations give surprisingly large values of free energies of solvation, which means the three ions could easily transfer from gas phase into water and dichloromethane. For all the three species, the ΔG_{elec} is the chief component to the ΔG_{solv}, implying that electrostatic interactions play an essential role in the solvation of the sandwich ionic species in the both solvents. The results might provide a reference to further explore these ionic species in solvents.

The solvent effects on the Gibbs free energies of the dissociate reactions for the ionic species in water and

Table 2 Reaction heat (ΔE, in kcal/mol), Gibbs free energy of reaction ($\Delta_r G$, in kcal/mol), and Gibbs free energy of reaction in water and dichloromethane at 298 K (ΔG^{solv}_{298K}, in kcal/mol) predicted at the B3LYP/6–311+G(d) level of theory

Dissociation reaction	ΔE	$\Delta_r G_{298K}$	$\Delta_r G^a$	$\Delta_r G^{solv}_{298K}$	
				H_2O	CH_2Cl_2
$[(Al_3N)_2K]^+ \rightarrow 2Al_3N + K^+$	12.3	−0.1	2.8	−25.1	−28.5
$[(Al_3N)ZnZn(Al_3N)]^{2+} \rightarrow [Zn_2(Al_3N)]^{2+} + Al_3N$	55.8	43.0	46.2	−6.7	−4.4
$[(Al_3N)ZnZn(Al_3N)]^{2+} \rightarrow 2\ [Zn(Al_3N)]^+$	7.4	−6.8	2.6	38.6	21.1
$[(Al_3N)Zn(C_5H_5)]^+ \rightarrow (C_5H_5)^- + Zn^{2+} + Al_3N$	493.6	473.3	477.9	65.1	155.5

[a] The Gibbs free energies were predicted at 223 K, except for the reaction $[(Al_3N)ZnZn(Al_3N)]^{2+} \rightarrow 2\ [Zn(Al_3N)]^+$ which was predicted at 103 K

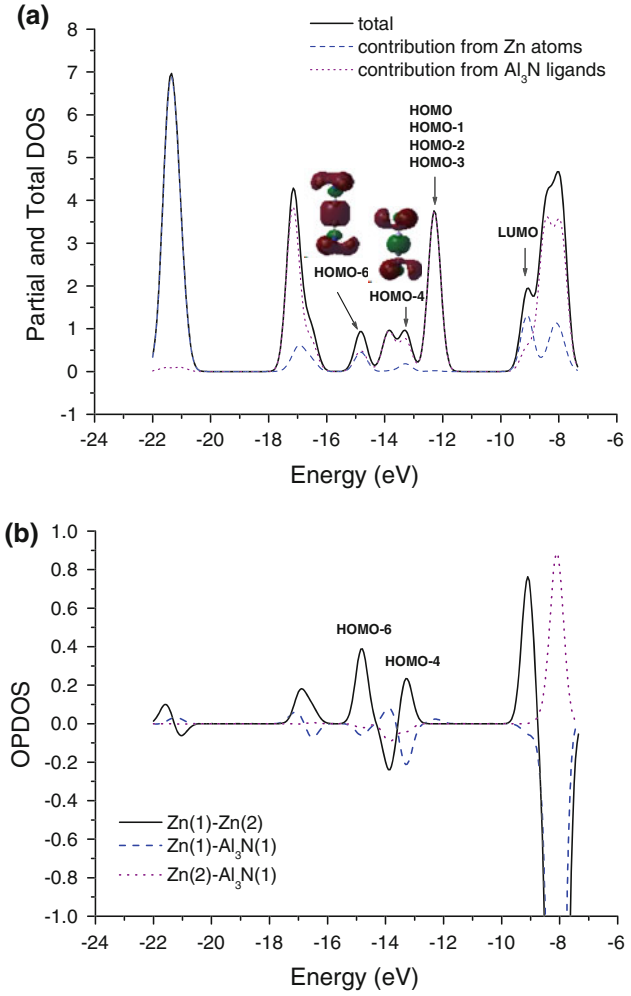

Fig. 3 **a** Density-of-states (DOS) spectrum and **b** overlap population density-of-states (OPDS) plot of D_{3d} $[(Al_3N)ZnZn(Al_3N)]^{2+}$ determined at the B3LYP/6–311+G(d) lever of theory. The *insets* display 3-D representations of the HOMO-4 and 6 with an isosurface contour value of 0.03

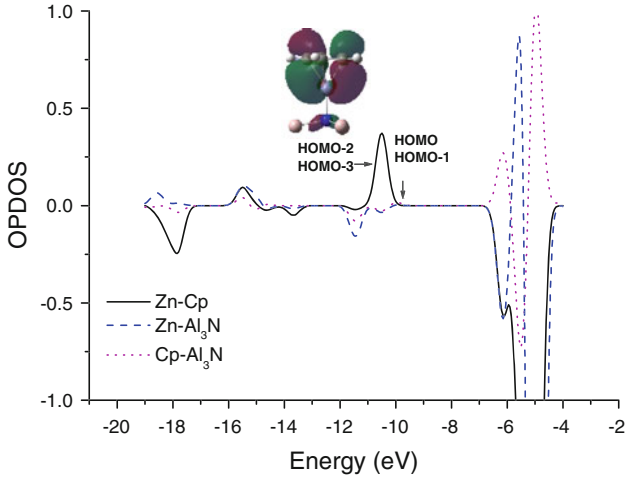

Fig. 4 Overlap population density-of-states (OPDS) plot of C_s $[(Al_3N)Zn(C_5H_5)]^+$ determined at the B3LYP/6–311+G(d) lever of theory. The *inset* display 3-D representations of the degenerate HOMO-2 and 3 with an isosurface contour value of 0.03

dichloromethane have also been considered. The two solvents have similar impact on the Gibbs free energy changes of the dissociate reactions. Table 2 shows that the solvent effect reduces the Gibbs free energies except for the reaction $[(Al_3N)ZnZn(Al_3N)]^{2+} \rightarrow 2\ [Zn(Al_3N)]^+$. For example, the $\Delta_r G_{298K}$ of the reaction of $[(Al_3N)_2K]^+ \rightarrow 2Al_3N + K^+$ is −0.1 kcal/mol in gas phase, while it decreases to −25.1 kcal/mol in water and −28.5 kcal/mol in dichloromethane, respectively, indicating that the solvents make $[(Al_3N)_2K]^+$ to dissociate more easily. The structure $[(Al_3N)ZnZn(Al_3N)]^{2+}$ is unstable either in gas phase or in solvents at room temperature. The dissociation $[(Al_3N)ZnZn(Al_3N)]^{2+} \rightarrow [Zn_2(Al_3N)]^{2+} + Al_3N$ occurs easily in solvents, while in gas phase the $[(Al_3N)ZnZn(Al_3N)]^{2+}$ tends to dissociate into $[Zn(Al_3N)]^+$ radicals. Although, the solvent effect significantly reduces the Gibbs free energy of the reaction $[(Al_3N)Zn(C_5H_5)]^+ \rightarrow (C_5H_5)^- + Zn^{2+} + Al_3N$ from 473.3 to 65.1 kcal/mol and 155.5 kcal/mol in water and dichloromethane, respectively, the dissociation is difficult to occur thermodynamically. Thus, we propose to synthesize stable salts of $[(Al_3N)Zn(C_5H_5)]^+$ containing Al_3N unit through the reverse reaction of the dissociation.

Table 3 The solvation energies (ΔG_{solv}, kcal/mol) of D_{3d} $[(Al_3N)K(Al_3N)]^+$, D_{3d} $[(Al_3N)ZnZn(Al_3N)]^{2+}$, and C_s $[(Al_3N)Zn(C_5H_5)]^+$ in water and dichloromethane, as well as the three components: free energies cavitation (ΔG_{cav}, kcal/mol), van der Waals term (ΔG_{vw}, kcal/mol), and electrostatic (ΔG_{elec}, kcal/mol)

Species	ΔG_{solv}		ΔG_{cav}		ΔG_{vw}		ΔG_{elec}	
	H_2O	CH_2Cl_2	H_2O	CH_2Cl_2	H_2O	CH_2Cl_2	H_2O	CH_2Cl_2
D_{3d} $[(Al_3N)K(Al_3N)]^+$	−23.8	−10.2	37.6	25.7	−3.0	−2.3	−58.4	−33.7
D_{3d} $[(Al_3N)ZnZn(Al_3N)]^{2+}$	−134.9	−88.3	35.5	26.0	−1.4	−1.2	−169.1	−113.2
C_s $[(Al_3N)Zn(C_5H_5)]^+$	−30.9	−23.2	25.9	19.0	−8.1	−7.3	−48.8	−35.0

4 Summary

This study shows that the D_{3h} Al_3N exhibits π aromaticity, and can be used as a ligand to construct three types of sandwich compounds, including traditional homo-decked sandwich, homo-decked binuclear sandwich, and hetero-decked sandwich. The $[(Al_3N)K(Al_3N)]^+$, $[(Al_3N)ZnZn(Al_3N)]^{2+}$, and $[(Al_3N)Zn(C_5H_5)]^+$ structures were designed as examples of the three types of sandwich compounds. These structures were predicted to be local minima on their corresponding potential hypersurfaces at the B3LYP, B3PW91, and BP86 levels of theory with the 6–311+G(d) basis set. In these designed sandwich complexes, the interaction between the Al_3N ligand and metal atoms are primarily electrostatic. The stabilities of the predicted molecules were checked by fragmentation. In gas phase, the $[(Al_3N)_2K]^+$ and $[(Al_3N)ZnZn(Al_3N)]^{2+}$ species are unstable at room temperature, while the $[(Al_3N)Zn(C_5H_5)]^+$ is very stable. The favored dissociation products of $[(Al_3N)ZnZn(Al_3N)]^{2+}$ in gas phase are $[Zn(Al_3N)]^+$ radicals, which are of great interesting because it is a novel stable Zn(I) compound. The solvent effects for the thermodynamics of the fragmentation reactions were investigated in water and dichloromethane. In both selected solvents, the decomposition reaction of the $[(Al_3N)K(Al_3N)]^+$ to K^+ and Al_3N is stronger than in gas phase. For the $[(Al_3N)ZnZn(Al_3N)]^{2+}$ species, the solvent effects appear to be unhelpful for stabilizing the sandwich structure, and the favored dissociation reaction is $[(Al_3N)ZnZn(Al_3N)]^{2+} \rightarrow [Zn_2(Al_3N)]^{2+} + Al_3N$. The $\Delta_r G_{298K}$ for the dissociation reaction of $[(Al_3N)Zn(C_5H_5)]^+$ to $(C_5H_5)^-$, Zn^{2+} and Al_3N are 473.3 kcal/mol in gas phase, 65.1 kcal/mol in water, and 155.5 kcal/mol in dichloromethane, respectively, indicating that the reverse reaction, namely the synthesis of $[(Al_3N)Zn(C_5H_5)]^+$, occurs easily. To our knowledge, this paper firstly proposes D_{3h} Al_3N could be used as a ligand in coordination chemistry. The designed species, especially the $[(Al_3N)Zn(C_5H_5)]^+$, expect the experimental verification in future.

Acknowledgments This research was supported in China by the National Natural Science Foundation of China (Grant No. 20802093 and 21003010), the scientific research fund of state key laboratory of explosion science and technology (Grant No. QNKT10-11 and 2DkT10–01a), Doctoral Fund of Ministry of Education of China (Grant No. 20070533142 and 20101101120032), Excellent talent training Fund of Beijing (Grant No. 2010D009011000003), Innovation Fund of explosive industry (Grant No. HZY09030104–5), Beijing Natural Science Foundation (Grant No. 2112036), China Postdoctoral Science Foundation (Grant No. 20100470558), and Excellent Young Scholars Research Fund of Beijing Institute of Technology (Grant No. 2009 Y1017).

References

1. Kroto HW, Heath JR, O'Brien SC, Curl RF, Smalley RE (1985) Nature 318:162
2. Guo BC, Kerns KP, Castleman AW Jr (1992) Science 255:1411
3. Khanna SN, Jena P (1992) Phys Rev Lett 69:1664
4. Khanna SN, Jena P (1995) Phys Rev B 51:13705
5. Kurikawa T, Takeda H, Hirano M, Judai K, Arita T, Nagao S, Nakajima A, Kaya K (1999) Organometallics 18:1430
6. Yang L, Ding Y, Sun C (2007) J Phys Chem A 111:10675
7. Reber AC, Khanna SN, Castleman AW Jr (2007) J Am Chem Soc 129:10189
8. de Heer WA (1993) Rev Mod Phys 65:611
9. Knight WD, Clemenger K, de Heer WA, Saunders WA, Chou MY, Cohen ML (1984) Phys Rev Lett 52:2141
10. Ekardt W (1984) Phys Rev B 29:1558
11. Ashman C, Khanna SN, Pederson MR (2000) Chem Phys Lett 324:137
12. Schleyer PVR (2005) Chem Rev 105:3433
13. Andrews L, Zhou M, Chertihin GV, Bare WD, Hannachi Y (2000) J Phys Chem A 104:1656
14. Li X, Wang LS (2005) Eur Phys J D 34:9
15. Averkiev BB, Boldyrev AI, Li X, Wang LS (2006) J Chem Phys 125:124305
16. Boo BH, Liu Z (1999) J Phys Chem A 103:1250
17. Jiang ZY, Ma WJ, Wu HS, Jin ZH (2004) Theochem 678:123
18. Wang B, Zhao J, Shi D, Chen X, Wang G (2005) Phys Rev A 72:023204
19. Nayak SK, Khanna SN, Jena P (1998) Phys Rev B 57:3787
20. Wright RJ, Brynda M, Power PP (2006) Angew Chem Int Ed 45:5953
21. Mercero JM, Piris M, Matxain JM, Lopez X, Ugalde JM (2009) J Am Chem Soc 131:6949
22. Becke AD (1993) J Chem Phys 98:5648
23. Lee C, Yang W, Parr RG (1988) Phys Rev B 37:785
24. Filatov M, Cremer D (2005) J Chem Phys 123:124101
25. Yanai Y, Tew DP, Handy NC (2004) Chem Phys Lett 393:51
26. Kobayashi R, Amos RD (2006) Chem Phys Lett 420:106
27. Kobayashi R, Amos RD (2006) Chem Phys Lett 424:225
28. Perdew JP, Burke K, Wang Y (1996) Phys Rev B 54:16533

29. Becke AD (1988) Phys Rev A 38:3098
30. Perdew JP (1986) Phys Rev B 33:8822
31. Frisch MJ, Pople JA, Binkley JS (1984) J Chem Phys 80:3265
32. Cossi M, Scalmani G, Rega N, Barone V (2002) J Chem Phys 117:43
33. Cammi R, Mennucci B, Tomasi J (2000) J Phys Chem A 104:5631
34. Frisch MJ, Trucks GW, Schlegel HB, Scuseria GE, Robb MA, Cheeseman JR, Montgomery JA Jr, Vreven T, Kudin KN, Burant JC, Millam JM, Iyengar SS, Tomasi J, Barone V, Mennucci B, Cossi M, Scalmani G, Rega N, Petersson GA, Nakatsuji H, Hada M, Ehara M, Toyota K, Fukuda R, Hasegawa J, Ishida M, Nakajima T, Honda Y, Kitao O, Nakai H, Klene M, Li X, Knox JE, Hratchian HP, Cross JB, Adamo C, Jaramillo J, Gomperts R, Stratmann RE, Yazyev O, Austin AJ, Cammi R, Pomelli C, Ochterski JW, Ayala PY, Morokuma K, Voth GA, Salvador P, Dannenberg JJ, Zakrzewski VG, Dapprich S, Daniels AD, Strain MC, Farkas O, Malick DK, Rabuck AD, Raghavachari K, Foresman JB, Ortiz JV, Cui Q, Baboul AG, Clifford S, Cioslowski J, Stefanov BB, Liu G, Liashenko A, Piskorz P, Komaromi I, Martin RL, Fox DJ, Keith T, Al-Laham MA, Peng CY, Nanayakkara A, Challacombe M, Gill PMW, Johnson B, Chen W, Wong MW, Gonzalez C, Pople JA (2003) Gaussian 03 revision C02. Gaussian, Pittsburgh
35. Gorelsky SI, AOMix program, rev. 5.62. http://www.obbligato.com/software/aomix
36. Gorelsky SI, Lever ABP (2001) J Organomet Chem 635:187
37. Glendening E, Badenhoop JK, Reed AE, Carpenter JE, Bohmann JA, Morales CM, Weinhold F (2001) NBO 5.0 program. University of Wisconsin, Madison
38. Seo DK, Corbett JD (2001) Science 291:841
39. Resa I, Carmona E, Gutierrez-Puebla E, Monge A (2004) Science 305:1136
40. Xie Y, Schaefer HFS, King RB (2005) J Am Chem Soc 127:2818
41. Xie Y, Schaefer HF, King RB (2000) J Am Chem Soc 122:8746
42. Wang H, Xie Y, King RB, Schaefer HF (2006) Inorg Chem 45:5621
43. Liao M, Zhang Q, Schwarz WHE (1995) Inorg Chem 34:5597
44. Kaupp M, von Schnering HG (1994) Inorg Chem 33:4179
45. Greene TM, Brown W, Andrews L, Downs AJ, Chertihin GV, Runeberg N, Pyykkö P (1995) J Phys Chem 99:7925
46. del Ri D, Galindo A, Resa I, Carmona E (2005) Angew Chem Int Ed 44:1244
47. Xie ZZ, Fang WH (2005) Chem Phys Lett 404:212
48. Yang L, Ding Y, Sun C (2007) J Am Chem Soc 129:1900